Available online at www.sciencedirect.com
ScienceDirect
Physics Letters B 658 (2007) 45–49
PHYSICS LETTERS B
www.elsevier.com/locate/physletb

Spectral properties of quarks above T_c in quenched lattice QCD

Frithjof Karsch [a], Masakiyo Kitazawa [b,*]

[a] *Brookhaven National Laboratory, Bldg. 510A, Upton 11973, NY, USA*
[b] *Department of Physics, Osaka University, Toyonaka, Osaka 560-0043, Japan*

Received 3 August 2007; accepted 9 October 2007

Available online 25 October 2007

Editor: J.-P. Blaizot

Abstract

We analyze the quark spectral function above the critical temperature for deconfinement in quenched lattice QCD using clover improved Wilson fermions in Landau gauge. We show that the temporal quark correlator is well reproduced by a two-pole approximation for the spectral function and analyze the bare quark mass dependence of both poles as well as their residues. In the chiral limit we find that the quark spectral function has two collective modes which correspond to the normal and plasmino excitations. At large values of the bare quark mass the spectral function is dominated by a single pole.

PACS: 11.10.Wx; 12.38.Aw; 12.38.Gc; 14.65.-q; 25.75.Nq

To explore the properties of hot and dense matter formed by quarks and gluons above the critical temperature for deconfinement (T_c) is an intriguing problem that has been addressed in many studies. Recent experimental results on the properties of the matter created in heavy ion collisions at the Relativistic Heavy-Ion Collider (RHIC) suggest, that its time evolution above T_c is well described by ideal hydrodynamics down to the freeze-out temperature in the vicinity of T_c [1]. In order to understand better the structure of matter in this non-perturbative region, it is desirable to identify the basic degrees of freedom of the system and their quasi-particle properties.

At asymptotically high temperatures almost free quarks and gluons are most certainly the basic degrees of freedom that control the properties of the Quark–Gluon plasma (QGP) [2]. In this regime properties of the QGP can be analyzed using perturbative techniques. At lower temperatures the application of hard-thermal loop (HTL) resummation [3] still allowed to define gauge independent propagators for quarks and gluons that can be used to study properties of the QGP perturbatively. From these perturbative analyses it is known that the collective excitations of gluons and quarks develop a mass gap (thermal mass) that is proportional to gT [2–4], where g and T denote the gauge coupling and temperature, respectively. Moreover, the number of poles in the finite temperature quasi-particle propagators is doubled. In addition to the normal modes, which reduce to poles in the free particle propagator, plasmon and plasmino modes appear.

At temperatures in the vicinity of T_c it is apriori not clear whether a quasi-particle picture for quarks and gluons is valid at all. However, lattice results on, e.g., baryon number and electric charge fluctuations in the vicinity of T_c [5] suggest that quasi-particles with quark degrees of freedom are the carriers of these quantum numbers. Quasi-particles also have been used successfully to describe lattice QCD results on the equation of state [6]. Moreover, the apparent quark number scaling of the elliptic flow observed in the RHIC experiments [7] may also suggest that quasi-particles with quark quantum numbers exist even close to T_c. Despite the problem of gauge dependence of quark and gluon propagators, it therefore is desirable to analyze their properties at high temperature through a direct calculation within the framework of QCD. In this Letter, we analyze dynamical properties of quarks above T_c in quenched lattice QCD. These calculations have been performed in Landau gauge. So

* Corresponding author.
E-mail addresses: karsch@quark.phy.bnl.gov (F. Karsch), kitazawa@phys.sci.osaka-u.ac.jp (M. Kitazawa).

0370-2693
doi:10.1016/j.physletb.2007.10.034

far, there have been only a few studies that address this problem in lattice calculations [8].

In order to understand the origin of the plasmino mode in the quark propagator in the high temperature limit, it is instructive to consider the quark propagator at intermediate temperature by introducing some energy scale of the order of the temperature [9–11]. In [9], the temperature dependence of the spectral function for fermions with scalar mass m has been considered in QED. In this model, the spectral function at zero temperature has two poles at energies $\omega = \pm m$, while in the high temperature limit, $T/m \to \infty$, it approaches the HTL result, which has four poles. The one-loop calculation performed in [9] clearly showed that the two limiting forms of the spectral function are connected continuously; in the spectral function a peak corresponding to the plasmino gradually appears and becomes larger with increasing temperature, in addition to the normal quasiparticle peak [9].

In this Letter, we analyze the quark propagator at two values of the temperature, $T = 1.5T_c$ and $3T_c$, as a function of the bare quark mass. To simplify the present analysis, all our calculations have been performed for zero momentum. The dynamical properties of quarks at zero momentum are encoded in the quark spectral function $\rho(\omega)$ which is related to the Euclidean correlation function

$$S(\tau) = \frac{1}{V}\int d^3x\, d^3y \left\langle \psi(\tau, \boldsymbol{x})\bar{\psi}(0, \boldsymbol{y})\right\rangle, \tag{1}$$

through an integral equation

$$S(\tau) = \int_{-\infty}^{\infty} d\omega \frac{e^{(1/2-\tau T)\,\omega/T}}{e^{\omega/2T} + e^{-\omega/2T}}\rho(\omega), \tag{2}$$

with the quark field ψ, the spatial volume V, and the imaginary time τ which is restricted to the interval $0 < \tau < 1/T$. The Dirac structure of $\rho(\omega)$ is decomposed as

$$\begin{aligned}\rho(\omega) &= \rho_0(\omega)\gamma^0 + \rho_{\rm s}(\omega)\\ &= \rho_+(\omega)\Lambda_+\gamma^0 + \rho_-(\omega)\Lambda_-\gamma^0,\end{aligned} \tag{3}$$

with projection operators $\Lambda_\pm = (1 \pm \gamma^0)/2$. The charge conjugation symmetry leads to $\rho_0(\omega) = \rho_0(-\omega)$, $\rho_{\rm s}(\omega) = -\rho_{\rm s}(-\omega)$, and $\rho_+(\omega) = \rho_-(-\omega) = \rho_0(\omega) + \rho_{\rm s}(\omega)$ [9,12]. In the following analysis, we concentrate on a determination of $\rho_\pm(\omega)$ instead of $\rho_{0,{\rm s}}(\omega)$, because excitation properties of quarks are more apparent in these channels [9]. In analogy to Eq. (3) we introduce the decomposition of the correlation function $S(\tau)$ as $S(\tau) = S_+(\tau)\Lambda_+\gamma^0 + S_-(\tau)\Lambda_-\gamma^0$, where $S_\pm$ are related through $S_+(\tau) = S_-(\beta - \tau)$.

For free quarks with scalar mass m_q the spectral functions, $\rho_\pm(\omega) = \delta(\omega \mp m_q)$, have quark and antiquark poles at $\omega = \pm m_q$, respectively. In the high temperature limit, additional poles, corresponding to the plasmino, appear at negative energy for $\rho_+(\omega)$ and positive energy for $\rho_-(\omega)$ [9,11,12]. While the positivity of $\rho_\pm(\omega)$ is ensured by definition, these spectral functions are neither even nor odd functions. In the chiral limit, however, $\rho_{\rm s}$ vanishes and $\rho_\pm(\omega)$ become even functions.

To extract the spectral function $\rho_+(\omega)$ from $S(\tau)$ using Eq. (2), we assume that $\rho_+(\omega)$ can be described by a two-pole ansatz,

$$\rho_+(\omega) = Z_1\delta(\omega - E_1) + Z_2\delta(\omega + E_2), \tag{4}$$

where the residues $Z_{1,2}$ and energies $E_{1,2} > 0$ have to be determined from a fit to $S_+(\tau)$. The poles at $\omega = E_1, -E_2$ correspond to the normal and plasmino modes, respectively [9].

Table 1
Simulation parameters [15]

T/T_c	N_τ	N_σ	β	$c_{\rm SW}$	κ_c	a [fm]
3	16	64, 48	7.457	1.3389	0.13390	0.015
	12	48	7.192	1.3550	0.13437	0.021
1.5	16	64, 48	6.872	1.4125	0.13495	0.031
	12	48	6.640	1.4579	0.13536	0.041

The correlation function $S(\tau)$ has been calculated at two values of the temperature, $T = 1.5T_c$ and $3T_c$, in quenched QCD using non-perturbatively improved clover Wilson fermions [13,14]. To control the dependence of our results on the finite lattice volume, $N_\sigma^3 \times N_\tau$, and lattice spacing, a, we analyze the quark propagator on lattices of three different sizes. The gauge field ensembles used for this analysis have been generated and used previously by the Bielefeld group to study screening masses and spectral functions [15]. The different simulation parameters are summarized in Table 1 [15]. For each lattice size, 51 configurations have been analyzed. On the $64^3 \times 16$ lattices and at our smallest temperature, $T = 1.5T_c$, we observed for the largest values of the hopping parameter, i.e., closest to κ_c, an anomalous behavior of the quark propagator on a few gauge field configurations. The appearance of such exceptional configurations in calculations with light quarks in quenched QCD is a well-known problem in calculations with Wilson fermions [16]. We identified 7 such configurations, which we excluded from our analysis. The properties of the quark propagator on these configurations will be discussed in more detail elsewhere [17]. Quark propagators have been calculated after fixing each gauge field configuration to Landau gauge. For this we used a conventional minimization algorithm with a stopping criterion, $(1/3)\,{\rm tr}\,|\partial_\mu A^\mu|^2 < 10^{-11}$. In the Wilson fermion formulation the bare mass, m_0, is related to the hopping parameter κ, through the standard relation

$$m_0 = \frac{1}{2a}\left(\frac{1}{\kappa} - \frac{1}{\kappa_c}\right), \tag{5}$$

where κ_c denotes the critical hopping parameter corresponding to the chiral limit, or vanishing quark mass.

To evaluate Eq. (1) numerically, we solve the linear equation $K\psi_{\rm result} = \psi_{\rm source}$ for a given source $\psi_{\rm source}$, with K being the fermion matrix. For this procedure, we use the wall source, $\psi^{\rm w}_{\rm source} = (1/V)\sum_x \psi(0, \boldsymbol{x})$, which we found to be very efficient in reducing the statistical error in the propagator calculation. To reduce the statistical error further, we define the correlation function $S_+(\tau)$ for each configuration by

$$S_+^{\rm latt.}(\tau) = \frac{1}{12}\,{\rm tr}\big[S(\tau)\gamma^0\Lambda_+ + S(\beta - \tau)\gamma^0\Lambda_-\big], \tag{6}$$

with the trace taken over Dirac and color indices.

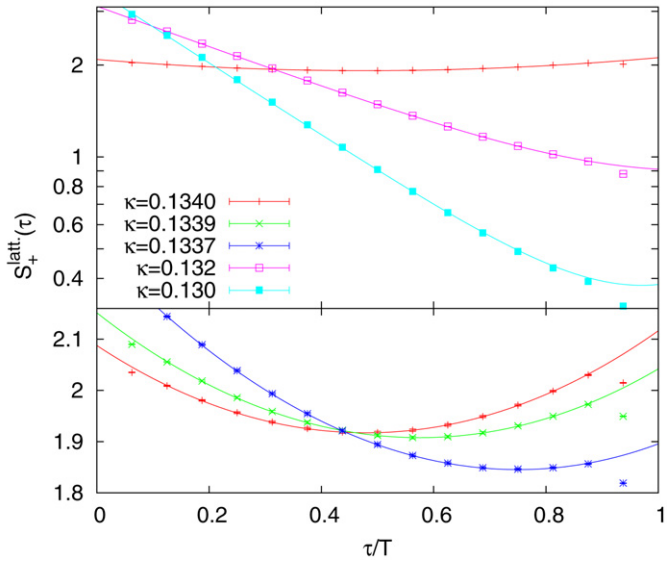

Fig. 1. The lattice correlation function $S_+^{\text{latt.}}(\tau)$ at $T = 3T_c$ for the lattice of size $64^3 \times 16$ with various values of κ, and the fitting result with the ansatz Eq. (4).

In Fig. 1, we show the numerical results for $S_+^{\text{latt.}}(\tau)$ for several values of κ calculated on a lattice of size $64^3 \times 16$ at $T = 3T_c$. One sees that the shape of $S_+^{\text{latt.}}(\tau)$ approaches that of a single exponential function for smaller κ, while it becomes symmetric as κ approaches κ_c. In the vicinity of the wall source, i.e., at small and large τ, we see deviations from this generic picture which can be attributed to distortion effects arising from the presence of the source. We thus exclude points with $\tau < \tau_{\min}$ and $N_\tau - \tau < \tau_{\min}$ from our fits to the ansatz given in Eq. (4). The resulting correlation functions obtained from correlated fits with $\tau_{\min} = 3$ are shown in Fig. 1. One sees that $S_+^{\text{latt.}}$ is well reproduced by our fitting ansatz[1]; the χ^2/dof of our fits is between 2 and 3 at $0.1335 \lesssim \kappa \lesssim 0.134$, while it gradually increases as κ becomes smaller than $\kappa = 0.1335$. A similar behavior is also observed for our other lattice sizes [17].

In Fig. 2, we show the dependence of $E_{1,2}$ and $Z_2/(Z_1+Z_2)$ on the bare quark mass m_0 for $T = 1.5T_c$ and $3T_c$. The results have been obtained from two-pole fits on lattices of size $64^3 \times 16$. Errorbars have been estimated from a Jackknife analysis. The dotted line in this figure denotes the pole mass determined from the bare lattice mass given in Eq. (5), i.e., $E_1/T = m_0/T = m_0 a N_\tau$. The figure shows that the ratio $Z_2/(Z_1 + Z_2)$ becomes larger with decreasing m_0 and eventually reaches 0.5. The hopping parameters satisfying $Z_1 = Z_2$ are $\kappa_c' = 0.133974(10)$ for $T = 3T_c$ and $\kappa_c' = 0.134991(9)$ for $T = 1.5T_c$, which are consistent with the values for κ_c given in Table 1. The latter had been obtained in [15] from a fit to critical hopping parameters determined in [14] from the vanishing of the isovector axial current. The numerical results obtained on $64^3 \times 16$ lattices show that E_1 and E_2 are equal within statistical errors at $\kappa = \kappa_c'$. The spectral function $\rho_+(\omega)$ thus becomes an even function at this point; the quark propagator

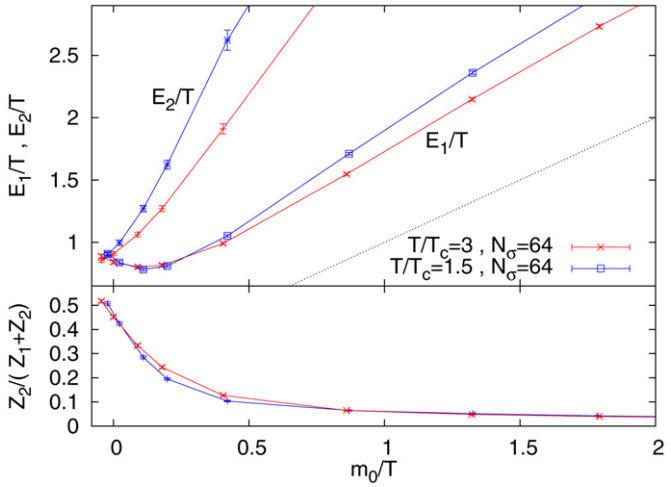

Fig. 2. The bare quark mass dependence of fitting parameters $E_{1,2}$ and $Z_2/(Z_1 + Z_2)$ at $T = 1.5T_c$ and $3T_c$ for lattice $64^3 \times 16$.

becomes chirally symmetric despite the presence of a thermal mass, $m_T \equiv E_1 = E_2$. From Fig. 2, one also finds that the ratio m_T/T is insensitive to T in the temperature range analyzed in this work, while it is slightly larger for lower T.

As m_0 becomes larger, $Z_2/(Z_1 + Z_2)$ decreases and $\rho_+(\omega)$ is eventually dominated by a single-pole. One sees that E_1 has a minimum at $m_0 > 0$, while E_2 is an increasing function of m_0. In the one-loop approximation, the peak in $\rho_+(\omega)$ corresponding to E_1 (E_2) is monotonically increasing (decreasing) function of m_0/T [9,17]. The quark mass dependence of poles found here thus is qualitatively different from the perturbative result. We find, however, that slope of E_2 as function of m_0/T decreases with increasing T. This may suggest that the perturbative behavior could eventually be recovered at much larger temperatures.

In order to check the dependence of our results on the lattice spacing and finite volume, we analyzed the quark propagator at $T = 3T_c$ for three different lattice sizes. Results for E_1 and E_2 are shown in Fig. 3. Comparing the results obtained on lattices with different lattice cut-off, a, but same physical volume, i.e., $64^3 \times 16$ and $48^3 \times 12$, one sees that any possible cut-off dependence is statistically not significant in our analysis. On the other hand we find a clear dependence of the quark energy levels on the spatial volume; when comparing lattices with aspect ratio $N_\sigma/N_\tau = 3$ and 4 we find that the energy levels, $E_{1,2}$, drop significantly. A similar behavior is observed also at $T = 1.5T_c$.

The presence of a strong volume dependence of the quark propagator is not unexpected. In fact, the thermal quark mass arises as collective effect of low momentum gluons; gluons at the soft scale $p \lesssim gT$ play a crucial role to give rise to the thermal mass at high temperatures [2,3]. However, on lattices with given aspect ratio N_σ/N_τ low momentum gluons are cut-off. The lowest non-vanishing gluon momentum is, $p_{\min}/T = 2\pi(N_\tau/N_\sigma)$, which still is larger than unity on lattices with aspect ratio $N_\sigma/N_\tau = 4$. The situation may, nonetheless, be somewhat better in the temperature range explored here as the temperature dependent coupling $g(T)$ is larger than unity. An analysis of quark spectral functions on lattices with

[1] We also checked that fits based only on a single pole ansatz lead to unacceptable large χ^2/dof.

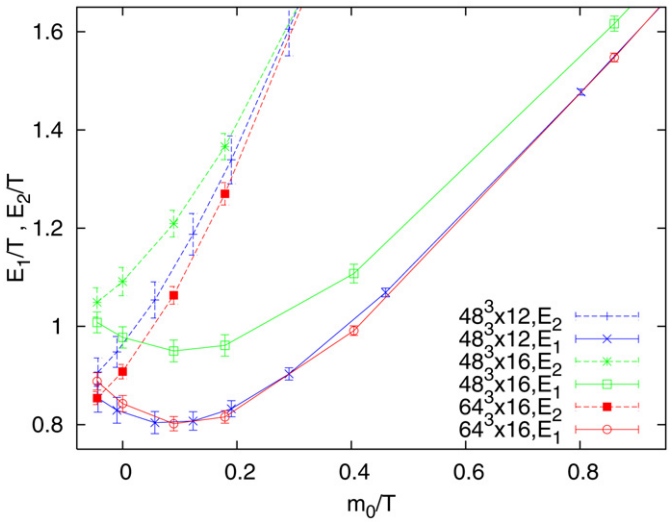

Fig. 3. The bare quark mass dependence of parameters E_1, E_2 at $T = 3T_c$ for lattices of size $64^3 \times 16$, $48^3 \times 16$ and $48^3 \times 12$.

even larger spatial volume is needed in the future to properly control effects of small momenta. We attempted to estimate the thermal mass in the $V \to \infty$ limit by extrapolating the results obtained for two different volumina. Defining $m_T \equiv (Z_1 E_1 + Z_2 E_2)/(Z_1 + Z_2)|_{\kappa=\kappa_c}$ and assuming the volume dependence of m_T as $m_T(N_\tau/N_\sigma) = m_T(0)\exp(cN_\tau^3/N_\sigma^3)$, we obtain $m_T(0)/T = 0.771(18)$ for $T = 3T_c$ and $m_T(0)/T = 0.800(15)$ for $T = 1.5T_c$. This suggests that finite volume effects may still be of the order of 15% in our current analysis of m_T/T. Despite these problems, our result clearly shows that light quarks near but above T_c have a mass gap that is of collective nature similar to that in the perturbative regime.

In this Letter, we analyzed the quark spectral function at zero momentum for $T = 1.5T_c$ and $3T_c$ as functions of bare quark mass m_0 in quenched lattice QCD with Landau gauge fixing. We found that the two-pole approximation for $\rho_+(\omega)$ well reproduces the behavior of the lattice correlation function. It is argued that the chiral symmetry of the quark propagator is restored at the critical value of κ and the shape of the spectral function at this point takes a similar form as in the high temperature limit having normal and plasmino modes with thermal mass m_T. As m_0 is increased, $\rho_+(\omega)$ approaches a single-pole structure as one can naturally deduce intuitively. The non-perturbative nature of thermal gauge fields is reflected in the behavior of poles as functions of m_0, which is qualitatively different from the perturbative result [9]. We also note that the ratio m_T/T decreases slightly with increasing T, which is expected to happen at high temperature where m/T should be proportional to a running coupling $g(T)$. Although results on the quark propagator are gauge dependent, we expect that our results for its poles suffer less from gauge dependence, because the success of the pole approximation for $\rho_+(\omega)$ indicates that the quark propagator has dynamical poles near the real axis, which are gauge independent quantities [9,18].

In the present study, we analyzed the quark spectral function in the quenched approximation. Although this approximation includes the leading contribution in the high temperature limit [2] and thus is valid at sufficiently high T, the validity of this approximation near T_c is nontrivial. For example, screening of gluons due to the polarization of the vacuum with virtual quark–antiquark pairs is neglected in this approximation. The coupling to possible mesonic excitations [19,20], which may cause interesting effects in the spectral properties of the quark [11], are not incorporated, either. The comparison of the quark propagator between quenched and full lattice simulations would tell us the strength of these effects near T_c.

In the future it will also be interesting to use results on the non-perturbative structure of quark propagators as input for phenomenological studies of the QGP phase. For example, thermal properties of the charm quark [17] should be useful for the understanding of properties of charmonia above T_c [19]. The thermal mass of light quarks can also be used to evaluate details of their dynamics [21].

Although in this Letter we limited our analysis to zero momentum, a proper analysis at finite momentum [17] is needed for the understanding of the entire quark spectral function. In particular, the confirmation of the existence of a minimum in the plasmino dispersion relation at finite momentum [4] clearly is a challenging problem. The exploration of the gluon propagator is also an important subject of further studies. To clarify the origin of the quark mass dependence of E_1 and E_2, which is qualitatively different from the perturbative result, as well as the T dependence of the thermal mass, are open questions for further numerical and analytic studies.

Acknowledgements

M.K. is grateful to S. Datta, W. Soeldner and T. Umeda for helping in getting started with his first lattice simulation. He also thanks S. Ejiri for discussions. The lattice simulations presented in this work have been carried out using the cluster computers ARMINIUS@Paderborn, BEN@ECT* and BAM@Bielefeld. In the early phase of this project M.K. has been supported by Special Postdoctoral Research Program of RIKEN. F.K. has been supported by contract DE-AC02-98CH10886 with the US Department of Energy.

References

[1] I. Arsene, et al., Nucl. Phys. A 757 (2005) 1;
B.B. Back, et al., Nucl. Phys. A 757 (2005) 28;
J. Adams, et al., Nucl. Phys. A 757 (2005) 102;
K. Adcox, et al., Nucl. Phys. A 757 (2005) 184.
[2] M. Le Bellac, Thermal Field Theory, Cambridge Univ. Press, Cambridge, England, 1996.
[3] R.D. Pisarski, Phys. Rev. Lett. 63 (1989) 1129;
E. Braaten, R.D. Pisarski, Nucl. Phys. B 337 (1990) 569;
E. Braaten, R.D. Pisarski, Nucl. Phys. B 339 (1990) 310.
[4] V.V. Klimov, Sov. J. Nucl. Phys. 33 (1981) 934, Yad. Fiz. 33 (1981) 1734;
H.A. Weldon, Phys. Rev. D 28 (1983) 2007.
[5] R.V. Gavai, S. Gupta, Phys. Rev. D 73 (2006) 014004;
S. Ejiri, et al., Phys. Lett. B 633 (2006) 275.
[6] M. Bluhm, et al., Phys. Rev. C 76 (2007) 034901;
J.P. Blaizot, et al., Phys. Rev. D 63 (2001) 065003, hep-ph/0303185, and references therein.
[7] R.J. Fries, et al., Phys. Rev. C 68 (2003) 044902.
[8] G. Boyd, et al., Nucl. Phys. B 385 (1992) 481;

P. Petreczky, et al., Nucl. Phys. B (Proc. Suppl.) 106 (2002) 513;
M. Hamada, et al., hep-lat/0610010.
[9] G. Baym, et al., Phys. Rev. D 46 (1992) 4043.
[10] D. Boyanovsky, Phys. Rev. D 72 (2005) 033004.
[11] M. Kitazawa, T. Kunihiro, Y. Nemoto, Phys. Lett. B 633 (2006) 269;
M. Kitazawa, T. Kunihiro, Y. Nemoto, Prog. Theor. Phys. 117 (2007) 103.
[12] H.A. Weldon, Phys. Rev. D 61 (2000) 036003.
[13] B. Sheikholeslami, R. Wohlert, Nucl. Phys. B 259 (1985) 572.
[14] M. Luscher, et al., Nucl. Phys. B 491 (1997) 344.
[15] F. Karsch, et al., Phys. Lett. B 530 (2002) 147;
S. Datta, et al., Phys. Rev. D 69 (2004) 094507, hep-lat/0312037.
[16] W.A. Bardeen, et al., Phys. Rev. D 57 (1998) 1633;
T.A. DeGrand, et al., Nucl. Phys. B 547 (1999) 259.
[17] F. Karsch, M. Kitazawa, in preparation.
[18] R. Kobes, G. Kunstatter, A. Rebhan, Nucl. Phys. B 355 (1991) 1.
[19] M. Asakawa, T. Hatsuda, Phys. Rev. Lett. 92 (2004) 012001;
S. Datta, et al., Phys. Rev. D 69 (2004) 094507;
T. Umeda, et al., Eur. Phys. J. C 39S1 (2005) 9;
G. Aarts, et al., arXiv: 0705.2198 [hep-lat].
[20] T. Hatsuda, T. Kunihiro, Phys. Rev. Lett. 55 (1985) 158.
[21] Y. Hidaka, M. Kitazawa, Phys. Rev. D 75 (2007) 011901;
Y. Hidaka, M. Kitazawa, Phys. Rev. D 75 (2007) 099901.